Favored Reaction Mechanism of Calcium-Dependent Phospholipase A(2). Insights from Density Functional Exploration

ARTICLE *in* THE JOURNAL OF PHYSICAL CHEMISTRY B · SEPTEMBER 2010

Impact Factor: 3.3 · DOI: 10.1021/jp1003819 · Source: PubMed

3 AUTHORS, INCLUDING:

Nino Russo
Università della Calabria
511 PUBLICATIONS **7,939** CITATIONS
SEE PROFILE

Marirosa Toscano
Università della Calabria
199 PUBLICATIONS **3,702** CITATIONS
SEE PROFILE

Favored Reaction Mechanism of Calcium-Dependent Phospholipase A_2. Insights from Density Functional Exploration

Monica Leopoldini, Nino Russo,* and Marirosa Toscano

Dipartimento di Chimica and Centro di Calcolo ad Alte Prestazioni per Elaborazioni Parallele e Distribuite-Centro d'Eccellenza MIUR, Università della Calabria, I-87030 Arcavacata di Rende (CS), Italy

Received: January 14, 2010; Revised Manuscript Received: June 21, 2010

The *sn*-2 acyl hydrolysis of phospholipids catalyzed by phospholipase A_2 (PLA_2) was investigated at the density functional B3LYP level. The PLA_2 active site is represented by quantum-chemical models that are based on available X-ray crystal structures. The two still controversial catalytic triad and calcium-coordinated oxyanion reaction mechanisms were considered. Tetrahedral intermediate formation in the first mechanism and the cleavage of the C−O bond in the second one are the rate-determining steps. Both mechanisms, in the gas phase and in the protein-like environment, yielded potential energy profiles with low energy barriers and consequently the comparison did not indicate a clear preference for one or the other path. An alternative mechanism, based on some corrections to the previously suggested ones, provides for an optional pathway for the enzyme activity.

Introduction

Interfacial enzymes[1–32] are responsible for the metabolism of nonpolar and amphiphilic substances like phospholipids, dietary fats, sterols, eicosanoids, and carotenoids. Interfacial enzymes, which access the substrate directly from the lipid−water interface to carry out the turnover cycle,[33–38] have evolved to deal with these kinds of aggregates in aqueous dispersions. Phospholipase A_2 (PLA_2, EC 3.1.1.4, phosphatide *sn*-2 acylhydrolases), found in numerous organisms including mammalian tissues, venoms, and plants, has been for a long time the prototype for the interfacial enzymology.

PLA_2 catalyzes the hydrolysis of the *sn*-2-ester bond in 1,2-diacylglycero-*sn*-3-phospholipids (Scheme 1), liberating free fatty acids, especially arachidonic acid, esterified to glycerol in phospholipids to be stored in membranes, which is the precursor of biologically active eicosanoids.[39] Most eicosanoids act as critical mediators in inflammation, blood clotting, control of vascular tone, renal function, reproductive systems, phospholipids digestion, and cell differentiation.

In addition, neuronal and neuroendocrine functions of eicosanoids have been discovered recently, and it has been postulated that eicosanoids may play wider important roles in intercellular signal transduction.[40–43]

So far, at least 19 enzymes possessing PLA_2 activity have been identified in mammals. The secretory PLA_2 ($sPLA_2$) family, including 10 isozymes, consists of low-molecular-weight Ca^{2+}-requiring secretory enzymes, which are implicated in several biological processes, such as inflammation, host defense, and atherosclerosis. The cytosolic PLA_2 ($cPLA_2$) family consists of three enzymes, among which $cPLA_2\alpha$ plays an indispensable role in arachidonic acid cascade. The Ca^{2+}-independent PLA_2 ($iPLA_2$) family contains two enzymes and may play a major role in membrane phospholipid remodeling. Finally, the platelet-activating factor (PAF) acetylhydrolase (PAF-AH) family represents a unique group of PLA_2 that contains four enzymes exhibiting unusual substrate specificity toward PAF and/or oxidized phospholipids.[44]

SCHEME 1: Reaction Catalyzed by PLA_2

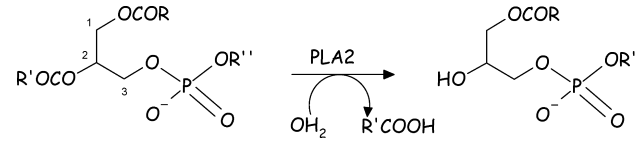

In view of this, inhibition or antagonism of the PLA_2 enzyme may constitute a fascinating approach for the design of new drugs against inflammation, arthritis, and rheumatism diseases.

The active site residues in all known sPLA2s are highly conserved.[45] The bovine pancreatic PLA_2 active site contains a Ca^{2+} ion coordinated by three carbonyl oxygen atoms coming from the Tyr28, Gly30, and Gly32 residues, by two oxygen atoms from Asp49, which acts as a bidentate ligand, and by two water molecules. The amide hydrogen atoms of Gly30 and Gly32 form hydrogen bonds with the phosphate group and the charged *sn*-2 group of the tetrahedral intermediate of the inhibitor/substrate during catalysis. The highly conserved His48 is located near the active site and is hydrogen bonded via nitrogen Nε2 to the likewise highly conserved Asp99.[46,47]

The Asp99-His48 pair has been suggested to play a key role in catalysis since the His48-Ala or Asp99-Ala mutants have less than 0.001% catalytic activity without a significant change in calcium binding or in the binding of the enzyme to the interface.[48]

Calcium ions prefer large and asymmetrical coordination geometries. Crystal structures of PLA_2 show that the active site calcium cation is usually heptacoordinated in a pentagonal bipyramid. In most calcium-containing enzymes the coordination number is seven, eight, or nine. Therefore, it is possible that the coordination sphere of the calcium in PLA_2 can be extended during catalysis from seven to eight or even nine ligands.[49]

On the basis of available crystal structures, Verheij et al. proposed a catalytic mechanism called the "catalytic triad mechanism" (see Scheme 2) because of its similarity to serine

* To whom correspondence should be addressed. E-mail: nrusso@unical.it.

10.1021/jp1003819
Published on Web 08/18/2010

SCHEME 2: Catalytic Triad (A) and Calcium-Coordinated Oxyanion (B) Reaction Mechanisms for PLA_2 Enzyme

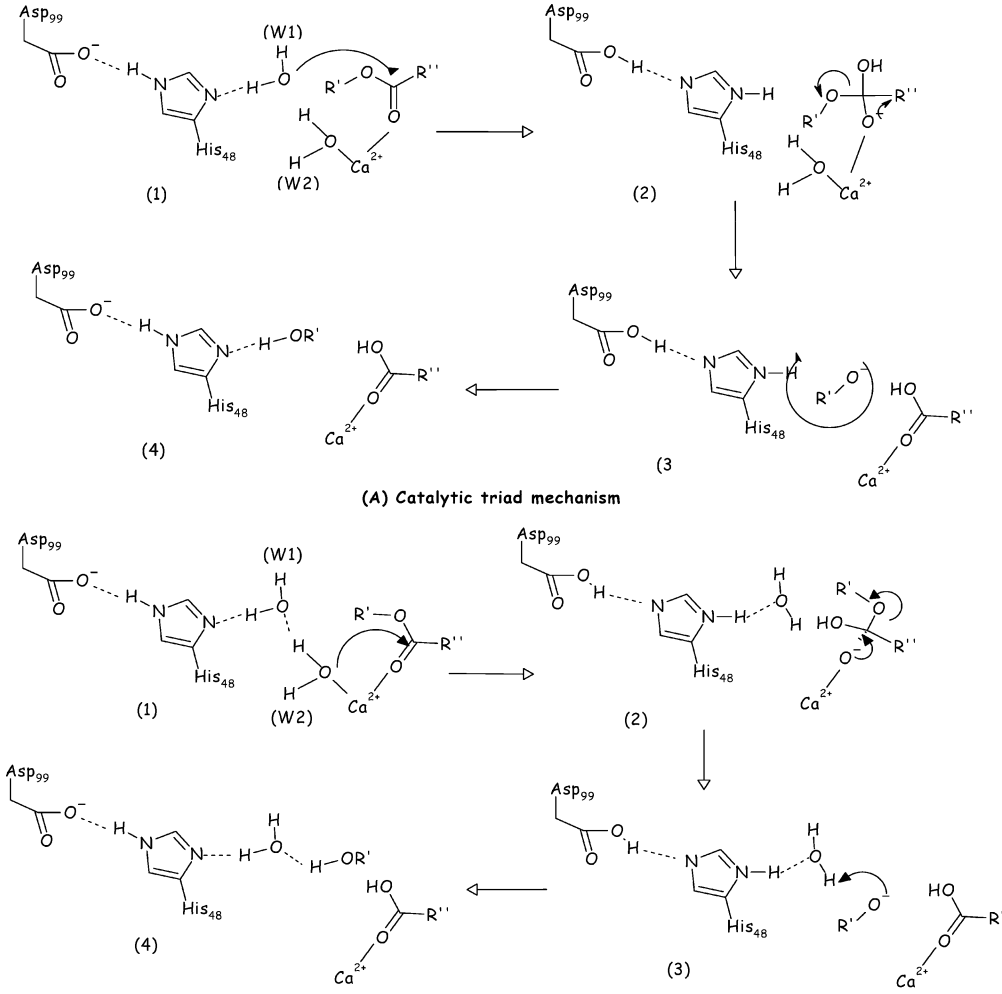

proteases enzymes.[50–52] Asp99, His48, and a water molecule (W1) present in the active site constitute a catalytic triad similar to the well-known Asp-His-Ser triad in serine proteases.[18,53] The nucleophilic attack by the water molecule of the triad on the carbonyl carbon of the *sn*-2 ester group of the substrate forms the tetrahedral intermediate. During this step, His48 is protonated at Nδ1 while the OH^- from H_2O is forming. The positively charged His48 is stabilized by the interaction with the negatively charged Asp99. The tetrahedral intermediate collapses into an alcoholate, which in turn is protonated by His48. According to this mechanism, the role of the calcium ion is to bind and to polarize the substrate, even if it is not involved directly in the catalysis.[50]

Recently, an alternative mechanism,[54–57] called the "calcium-coordinated oxyanion", has been suggested (see Scheme 2) on the basis of the flexibility of the calcium coordination and on kinetic studies with different head groups.[55] This mechanism differs from the former since it involves two different water molecules. One (W2) is coordinated to Ca^{2+} and it is deprotonated in order to give the nucleophile OH^- by the other water molecule, which in turn is hydrogen bonded to His48. This Ca^{2+}-bonded water performs the nucleophilic addition on the substrate, giving rise to the tetrahedral intermediate. This is protonated by the other water molecule with the help of the His/Asp pair, yielding to the products. In this case, the role performed by the cation is not only binding and polarizing the substrate, but also generating the nucleophile.

To design specific antiinflammatory, antiarthritic, and antirheumatic agents using PLA2 as a target molecule, it is highly desirable to obtain detailed information about the catalytic mechanism followed by PLA_2 enzyme. So, with the aim to determine which one may represent the more reliable reaction path among the two proposals, we have performed a density functional based study on lipid hydrolysis using a simplified model for the PLA_2 active site.

Method

All the computations were carried out with the Gaussian 03 code.[58] The hybrid Becke exchange and Lee, Yang, and Parr correlation (B3LYP) functional was used to perform geometry optimization.[59–62] The 6-311G** basis set was chosen for the C, N, O, P, and H atoms,[63–66] while for the metal the SDD pseudopotential in connection with the relative orbital basis set[67] was used.

Geometry optimization was followed by frequency calculations, performed on all stationary points of the reaction paths, to evaluate their character as minima or saddle points and to compute zero-point energy corrections, which were then included in all the relative energy values.

Single-point energy calculations using the 6-311++G** basis set were performed on the B3LYP/6-311G** optimized geometries and used to build the potential energy surfaces (PESs).

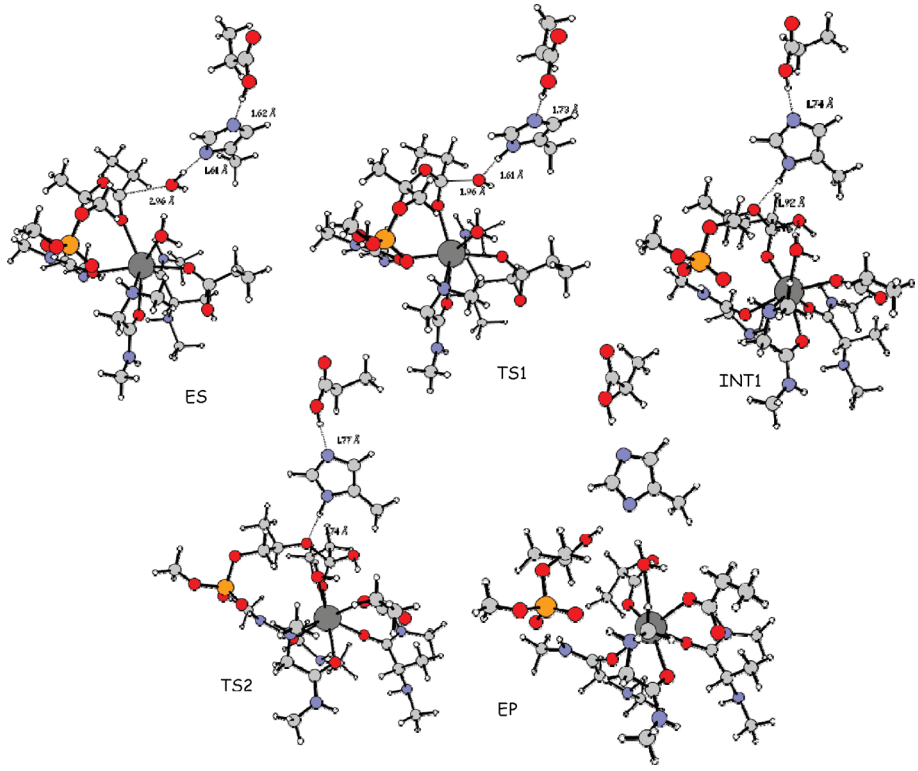

Figure 1. B3LYP-optimized geometries within the catalytic triad mechanism.

Intrinsic reaction coordinate (IRC) calculations[68,69] were performed with the aim to confirm that a given transition state connects a particular couple of consecutive minima.

The performance of the B3LYP functional in predicting properties of transition metals containing systems is supported by a large number of publications, especially concerning enzymatic catalysis[70–81] in which also hydrolysis reactions are involved.[76–81]

Solvent effects were introduced as single-point computations on the optimized gas-phase structures in the framework of self-consistent reaction field polarizable continuum model (SCRF-PCM)[82–84] in which the cavity is created via a series of overlapping spheres, using the PCM approach. The united atom (UA0) topological model applied on the atomic radii of the UFF force field[85] was used to build the cavity in the gas-phase equilibrium geometry. The dielectric constant value $\varepsilon = 4$ was chosen by taking into account the coupled effect of the protein itself and the water medium surrounding the protein, according to previous suggestions.[70–81] Other dielectric constants such as $\varepsilon = 2$, 40, and 80 were employed in these calculations, as discussed in the text.

The relative solvent effects between minima and transition states are normally calculated to be quite small, within 2−3 kcal/mol.[70,71]

The quantum mechanical (QM) studies performed on metalloenzymes use chemical models for the active sites since proteins are macromolecules not possible to be studied on the whole by theoretical methods. By use of available X-ray structures available for the enzyme and/or the complexes between it and substrate/inhibitors, the active site must be divided into two parts, the quantum mechanical cluster and the environment, which is the portion surrounding the catalytic region not involved in catalysis.

The quantum mechanical cluster is usually made up by the metal ion and its first coordination sphere, to which some nearby residues recognized as fundamental in catalysis are added. Ligands are represented by the functional part of the side chains only (imidazole rings for histidines, acetates for aspartates or glutamates). An atom of each amino acidic residue is usually kept frozen at its crystallographic position in order to mimic the steric effects produced by the surrounding protein and to avoid an unrealistic expansion of the cluster during the optimization procedure.[70–81] The substrate is left free from constraints during the optimization procedure.

The environment not explicitly included in the quantum cluster has a double steric and electrostatic effect. The first one can be brutally reproduced by fixing some crystallographic positions. The electrostatic effect is introduced assuming it being a homogeneous polarizable medium with a dielectric constant usually chosen to be equal to 4.

The active site model cluster used in this work was built starting from the 2.0 Å X-ray structure of the human phospholipase A_2 complexed with a substrate analogue (PDB code 1KVO).[86] The cluster is made up by a calcium(II) cation, three $CH_3NHCH_2CONHCH_3$ groups that mimic the Tyr28, Gly30, and Gly32 residues as far as the amide carbonyl moiety is involved in calcium coordination, two $CH_3CH_2COO^-$ groups that mimic the Asp49 and Asp99 residues, a methylimidazole as model for His48 amino acid, two water molecules, and a $[(CH_3OPO_2OCH_2CH(OCOCH_2CH_3)CH_3]^-$ as simplified substrate instead of the general $(RCOOCH_2CH(OCOR')CH_2OPO_2R'')^-$ phospholipid.

All geometries are available as Cartesian coordinates upon request.

Results and Discussion

Catalytic Triad Reaction Path. The stationary points belonging to the catalytic triad reaction path schematically reported in the Scheme 2 obtained as far as B3LYP computations are performed are presented in the Figure 1.

The first point encountered on the reaction path is the enzyme−substrate complex, ES, that occurs when the substrate

coordinates to the calcium cation through its carbonyl oxygen atom at 2.50 Å. Ca(II) results to be hepta-coordinated with the carbonyl oxygen from Tyr28 (2.45 Å), Gly30 (2.43 Å), and Gly32 (2.46 Å), the latter also establishing a coordination bond to the cation (2.55 Å) through the amide NH, and a H-bond with the substrate negative phosphate oxygen (1.78 Å). Asp49 acts as monodentate ligand (2.45 Å), while the water molecule W2 completes the coordination.

It is worth noting that, during the B3LYP geometry optimization of the ES complex, the His48 Nε hydrogen spontaneously shifts on the negative carboxylic oxygen of Asp99 without passing a barrier, yielding to a neutral carboxylate and a negative methylimidazole ring. However, the Asp99 proton exhibits a very long O−H bond length (1.09 Å) forming with His48 a very strong hydrogen bond (1.62 Å). This could be an artifact of the model used in the current study since in our calculations we have completely neglected the surrounding of Asp99 residue. Optimization of the enzyme active site without bound substrate at B3LYP level yields similar results; that is, a shift of the proton from His to Asp occurs. Employing a different DFT functional in ES geometry optimization does not alter notably the conclusions about the ES features. The MPWB1K functional[87] locates on the potential energy surface two minima for the ES complex, one for a negative Asp and a neutral His, and another one with a negative His and a neutral Asp. The former is found at 5.0 kcal/mol above the latter, so that the protonation scheme His^---AspH is slightly favored also at the MPWB1K level. The transition state in going from the first minimum to the other is computed to require only 1.7 kcal/mol. Considering the results obtained as far as the MPWB1K functional is concerned, the arrangement for the ES complex reported in the Figure 1 may be considered quite reliable, even if it is not so usual to find this protonation scheme for the pair His-Asp. This negative His residue involved into a strong H-bond with Asp99 seems to be just quite reactive to accept the proton from the catalytic water during the nucleophilic addition.

W1 is hydrogen bonded to His48 (1.61 Å) and lies at 2.96 Å from the substrate carbonyl carbon atom.

It can be seen from the ES geometry reported in the Figure 1 that the substrate in the reactants complex is found to be in a perfect position for nucleophilic attack by W1 and W2 (calcium-coordinated oxyanion mechanism).

Nucleophilic addition on the substrate carbonyl carbon coupled with the W1 deprotonation by His48 (TS1) occurs when the O(W1)-C(substrate), the O(W1)--H, and the H---Nδ(His48) distances assume the values of 1.96, 1.61, and 1.07 Å, respectively. In this stationary point, which was confirmed to be a first-order saddle point with only one imaginary frequency at 150 cm^{-1}, the calcium(II) maintains its heptacoordination with Tyr28 (2.47 Å), Gly30 (2.42 Å), Gly32 (2.50 and 2.57 Å), and Asp49 (2.37 Å) residues, with W2 (2.48 Å), and with the substrate oxygen (2.36 Å).

From this transition state, a stable intermediate (INT1) originates. The HO−C bond is completely formed (1.49 Å), the His48 amino acid is protonated at the Nδ position (1.03 Å), and it is involved into a H bond with the ester oxygen atom in the substrate (1.92 Å). So, His48 is well oriented to perform the protonation of the ester oxygen atom that should lead to the decomposition of the intermediate. The H bond in the pair His48−Asp99 is also retained in the INT1 (1.74 Å).

After this intermediate, the reaction passes through a transition state (imaginary frequency at 139 cm^{-1}), TS2, in which the O--C ester bond in the phospholipid substrate is breaking (critical distance is 1.79 Å) and in the meantime the proton is shifting from the Nδ atom in the His48 to the ester oxygen in the substrate (distances are 1.04 and 1.74 Å, for N−H and H−O, respectively).

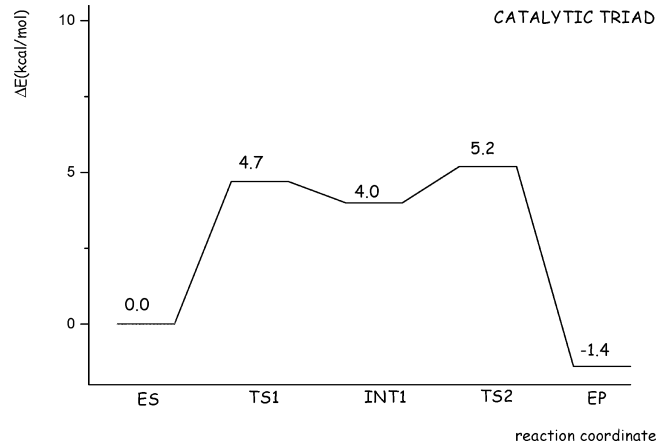

Figure 2. B3LYP potential energy surface (PES) for catalytic triad mechanism.

All the attempts devoted to the localization on the potential energy surface of an intermediate with unprotonated alcoholate failed, so that dissociation of the tetrahedral intermediate may occur in a concerted fashion.

The final optimized products complex, EP, shows a completely hydrolyzed ester substrate that results to be protonated (O−H bond is 0.98 Å). The OH group establishes a H bond with the negative Nδ atom of His48 (2.03 Å) that in turn receives a further hydrogen bond from the calcium-coordinated W2 (1.79 Å). Asp99 is again involved into a strong H bonding interaction with the negative His48 residue (at 1.68 Å). The hydrolyzed carboxylic acid is bound to the Ca(II) cation through the carbonyl oxygen at 2.52 Å.

The overall B3LYP energy diagram for the hydrolysis of the phospholipid model by the PLA_2 active site as far as the catalytic triad mechanism is concerned is shown in Figure 2. The first step of the reaction, that is, the nucleophilic attack on the substrate carbonyl carbon atom by W1 coupled to its deprotonation performed by His48, exhibits in the gas phase a very low energy barrier of 4.7 kcal/mol, suggesting that the catalytic triad His48-Asp99-W1 is very efficient in performing the water attack on the substrate so giving rise to the formation of the tetrahedral intermediate INT1 which lies at 4.0 kcal/mol with respect to the reactants complex. The decomposition of the INT1 species, mediated by the protonation of the ester oxygen by the His48 residue, presents a computed gas-phase energy barrier (TS2) of 1.2 kcal/mol, with respect to the INT1 species. Finally, products complex EP is found 1.4 kcal/mol below the reference.

The energy profile for the catalytic triad mechanism, computed at the MPWB1K level, is quite similar with that obtained using the B3LYP functional. TS1 is found at 3.9 kcal/mol with respect to the ES reactant complex, so giving again a very feasible barrier. INT1 and TS2 stationary points lie at 3.5 and 3.4 kcal/mol, and thus the tetrahedral intermediate easily collapses into the EP product complex, which is found 7.1 kcal/mol lower than the asymptote.

In the catalytic triad mechanism, the rate-limiting step seems to be the formation of the tetrahedral intermediate during which the Nδ in His48 is protonated, while its decomposition results to be energetically less demanding.

The pair His48-Asp99 is crucial for the catalysis. Particularly, His48 constitutes the catalytic base that allows the W1 deprotonation and, consequently, the nucleophile agent generation.

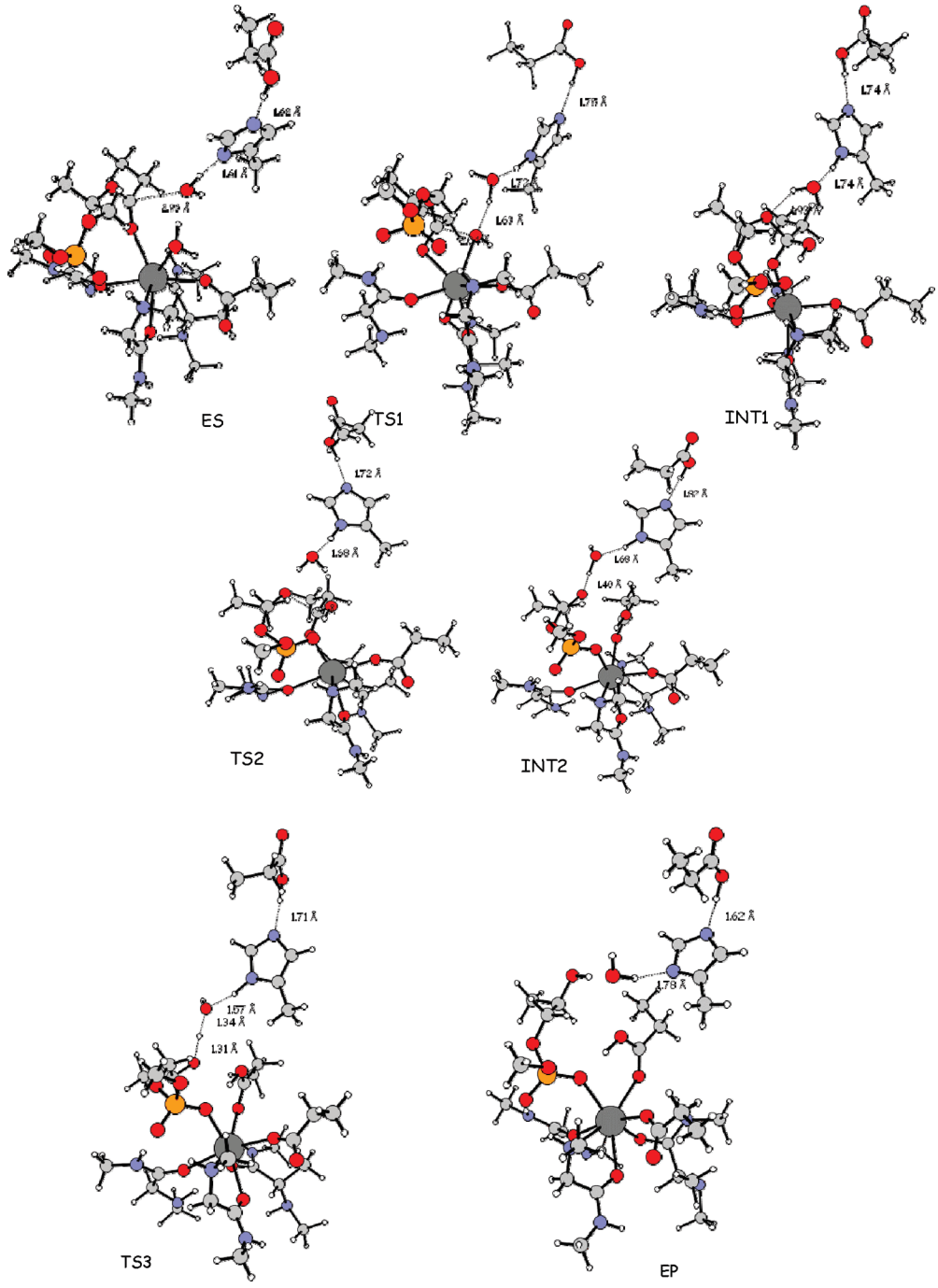

Figure 3. B3LYP-optimized geometries within the calcium-coordinated oxyanion mechanism.

These results account for the experimental finding of the dramatic loss of activity of the His48-Gln mutant.[88]

The other water molecule, W2, which is retained as calcium ligand through all the reaction, is useful for the stabilization of transition states and intermediates through formation of a H bonding network.

Calcium-Coordinated Oxyanion Reaction Path. The stationary points for the calcium-coordinated oxyanion reaction path obtained by B3LYP computations are depicted in Figure 3.

In this mechanism, the calcium-coordinated oxyanion is formed by the attack on the substrate carbonyl carbon by the equatorial Ca-bound W2, connected to Nδ of His48 through W1.

The nucleophilic attack by W2 occurs through the transition state TS1, characterized by an imaginary frequency at 149 cm^{-1}. In this saddle point, the O(W2)--C bond is forming (2.04 Å), W2 is being deprotonated by W1 (O(W2)--H and H--O(W1) distances are 1.63 and 1.02 Å) and W1 is being deprotonated by the Nδ of His48 (O(W1)---H and H---N(His48) distances are 1.72 and 1.05 Å). The vibrational normal mode mainly shows the movement of the heavy atoms during the proton transferring.

The tetrahedral intermediate INT1 presents a HO−C bond of 1.45 Å. W1 is hydrogen bonded to the oxygen atoms of the hydroxyl (1.87 Å) and the ester moiety (1.93 Å), and receives a further H bond from His48 (1.74 Å), which in turn interacts with Asp99 (1.74 Å). Another feature of this adduct is that Ca(II) loses a coordination (namely W2), remaining hexacoordinated in a distorted octahedral geometry (see Figure 3).

A second transition state, TS2, having an imaginary frequency of 152 cm^{-1}, is responsible for the cleavage of the O−C bond

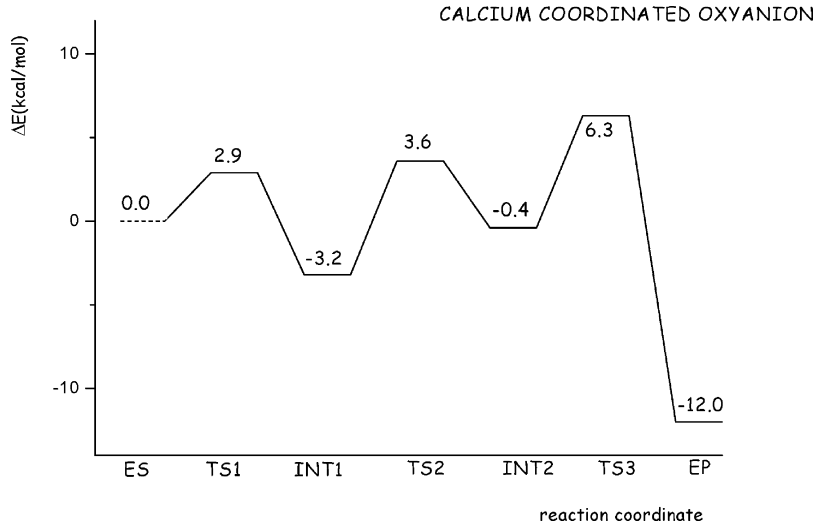

Figure 4. B3LYP potential energy surface (PES) for the calcium-coordinated oxyanion mechanism.

(critical distance is 1.93 Å) in the ester moiety of the substrate but not for its protonation (as occurred for the TS2 in the catalytic triad mechanism).

From the TS2, the INT2 species arises. The alcoholate is strongly H bonded to W1 (1.40 Å) that receives a H bond from the Nδ of His48 (1.68 Å). The carboxylic acid product is coordinated at 2.49 Å to Ca(II) that gains again a coordination through the phosphate group of the ester (2.38 Å).

The transition state TS3 entails the protonation of the alcoholate by W1 (O(alcoholate)--H(W1) and H--O(W1) critical distances are 1.31 and 1.34 Å, respectively), the latter being protonated by the Nδ of His48 (O(W1)--HN(His48) distance is 1.57 Å), and finally leading to the products complex. The heptacoordination around the calcium cation is retained in going from INT2 to TS3 to EP.

The potential energy profile within the calcium-coordinated oxyanion mechanism is depicted in the graph of Figure 4. As can be immediately seen from the reaction profile, the rate-limiting step can be now recognized in the tetrahedral intermediate decomposition, as supposed previously.[54–57]

The TS1 for the W2 nucleophilic addition on the carbonyl carbon atom requires an activation energy of only 2.9 kcal/mol and leads to the tetrahedral intermediate INT1 that lies 3.2 kcal/mol below the ES complex. The TS2, in which the C--O bond in the ester moiety of the tetrahedral intermediate is breaking, is found at 3.6 kcal/mol above the reference, so demanding a gas-phase energetic barrier of 6.8 kcal/mol. The INT2, characterized by a negative alcoholate, is found 0.4 kcal/mol below the ES state. It evolves toward the TS3, in which the alcoholate is protonated by the W1 with an energy barrier of 6.7 kcal/mol in vacuo.

The products complex lies 12.0 kcal/mol below the reference.

The results presented in the Figure 4 confirm that the calcium-coordinated oxyanion mechanism is also energetically possible. However, protonation of the tetrahedral intermediate performed by W1 with the help of His48 requires an amount of energy (6.8 and 6.7 kcal/mol, for TS2 and TS3, respectively) that is higher than the one involved in the nucleophilic addition step (2.9 kcal/mol). These findings indicate that calcium-coordinated water molecule (W2) is an excellent nucleophile in performing the attack on the carbonyl carbon since a very low barrier is involved in this step and that probably W1 could not be so acidic to protonate the ester oxygen atom in the intermediate.

The nucleophilic attack step requires an activation energy of 4.7 and 2.9 kcal/mol, according to the involvement of W1 (catalytic triad) and W2 (calcium-coordinated oxyanion) nucleophiles. The difference in the energy barriers indicates that the coordination of the W2 water molecule to the Ca(II) enhances its nucleophilic character with respect to the no metal coordination situation (the case of W1 in the catalytic triad mechanism). The tetrahedral intermediate protonation process, and thus its decomposition into products, occurs with an energy expense of 1.2 kcal/mol, and of 6.8 and 6.7 kcal/mol, depending on whether it is performed by the His48 amino acid alone or by the His48 with the involvement of W1, in the catalytic triad or calcium-coordinated oxyanion mechanism, respectively.

Calcium-Coordinated Catalytic Triad Reaction Path. In this study, we hypothesize another catalytic mechanism followed by the PLA_2 enzyme, simply by revising the literature proposal, and proposing a mixture of those already existing. According to this suggestion, calcium-bound W2 should perform the nucleophilic attack on the substrate, as occurring in the calcium-coordinated oxyanion mechanism, leading to the formation of a tetrahedral intermediate that, once protonated by His48 without the mediation of W1, collapses into products. W1 should just have an active role only during the formation of the tetrahedral intermediate, and a stabilization effect on transition states and intermediates originating during the tetrahedral decomposition.

The new reaction sequence is depicted in Scheme 3. The relative optimized structures of the stationary points are depicted in Figure 5.

The stationary points ES and TS1 are the same as those belonging to the calcium-coordinated oxyanion energy profile. But now, in the intermediate, INT1′, originating from the W2 attack on substrate (C−OH bond distance is 1.52 Å) a direct interaction between the hydrogen present on Nδ of His48 and the ester oxygen atom in the substrate (2.22 Å) occurs, as in the catalytic triad energy profile. W1 rearranges itself as to establish a H-bond with the O atom in the substrate (1.84 Å).

INT1′ decomposition into the products occurs through the transition state TS2′ (see Figure 5), in which the cleavage of the O−C ester bond in the substrate (1.99 Å) is coupled to the proton transfer from His48 to the ester oxygen (H--N and H--O distances are 1.06 and 1.77 Å, respectively). The vibrational normal mode, whose imaginary frequency is 124 cm^{-1}, mainly corresponds to the reaction coordinate describing the C−O bond breaking. The W1 is involved into a strong H-bond with the negative ester oxygen at 1.76 Å.

The final complex between enzyme active site and products (EP′) appears to be very similar to the one belonging to the

SCHEME 3: Calcium-Coordinated Catalytic Triad Mechanism (C) Proposed in This Study for PLA_2 Enzyme

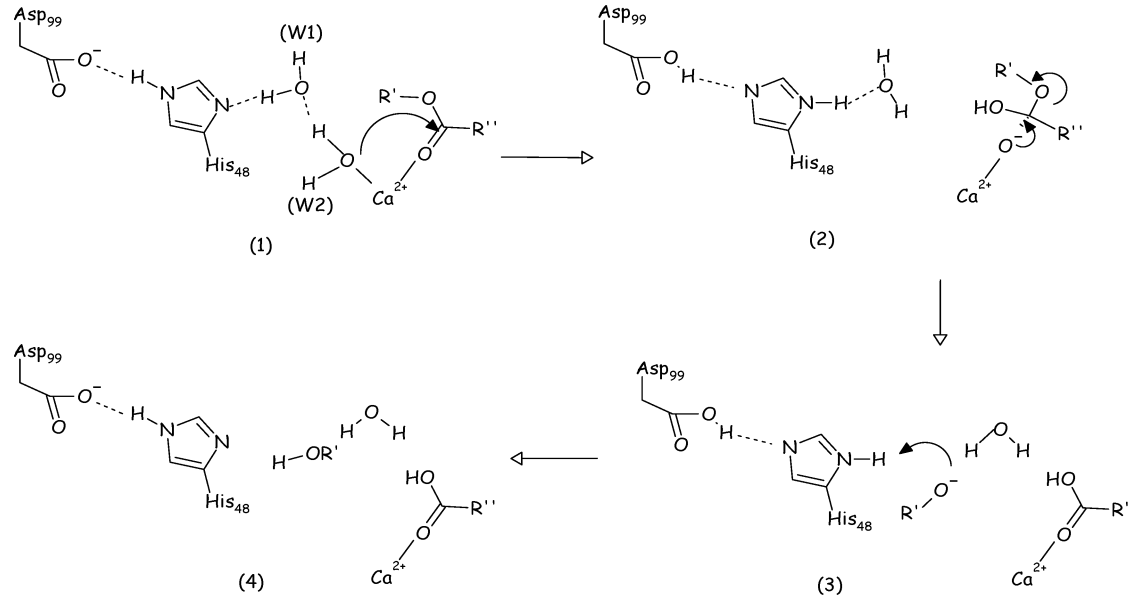

calcium-coordinated oxyanion energy profile. The only significant difference is the position and the orientation of the W1 molecule that acts as H-bond donor with the Nδ of His48 (1.85 Å) and the alcohol oxygen atom (2.22 Å). Hydrolysis products are both coordinated to the calcium cation at 2.43 and 2.60 Å, for the alcohol and the fatty acid, respectively.

The potential energy profile within the calcium-coordinated catalytic triad mechanism is depicted in the graph of Figure 6. The TS1 relative energy is the same as that of the calcium-coordinated oxyanion energy profile (2.9 kcal/mol), but now the tetrahedral intermediate INT1′ with the His48 pointing directly toward the substrate oxygen is found 6.1 kcal/mol below the reference. This value indicates that the absence of the W1 in the first coordination sphere of calcium entails a certain stabilization of the tetrahedral intermediate.

TS2′ relative energy is found to be 3.0 kcal/mol below the ES one, and the overall barrier for the tetrahedral decomposition step is calculated to be 3.1 kcal/mol, once the INT1′ state is reached. This finding underlines how His48 is a good candidate in acting as general acid catalyst and thus performing the breaking of the C−O bond in the intermediate.

The products complex, EP′, is found at 6.9 kcal/mol below the reference.

The potential energy curve reported in the Figure 6 shows how tetrahedral intermediate formation as well as its decomposition requires similar energy barriers (2.9 and 3.1 kcal/mol, respectively), so that the difference is too small to be able to unambiguously distinguish which one of them is the rate-limiting step within this mechanism. Another significant feature is that calcium-bound water molecule is a good nucleophilic agent, as encountered in calcium-coordinated oxyanion path, and the His48 can thus be considered crucial for the ester bond cleavage in the substrate.

Solvent Effects. To account for the protein that is not explicitly included in model cluster, we have assumed the surrounding as a homogeneous polarizable medium. This approximation has been used frequently in several computational works on enzymes.[70–81]

First, the typical dielectric constant $\varepsilon = 4$ has been chosen for calculations, according to previous suggestions.[70–81] However, since PLA_2 is an interfacial enzyme whose active site should be quite accessible to water, a better description of the

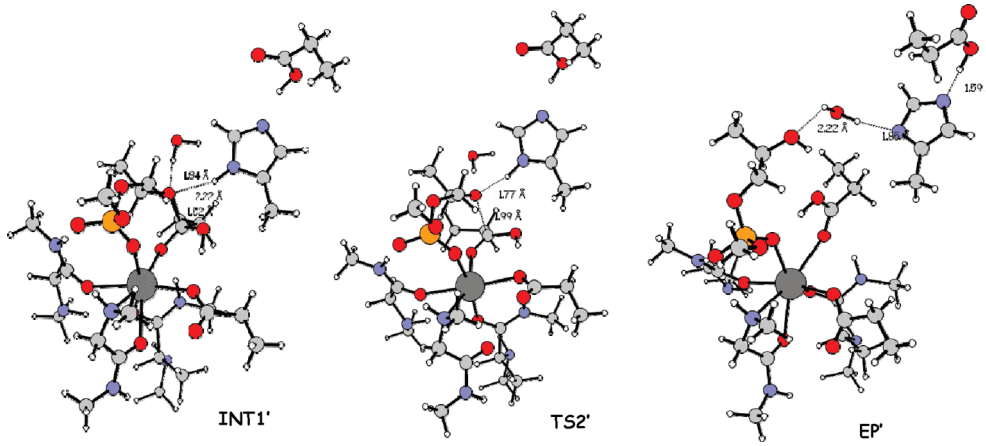

Figure 5. B3LYP-optimized geometries within the calcium-coordinated catalytic triad mechanism.

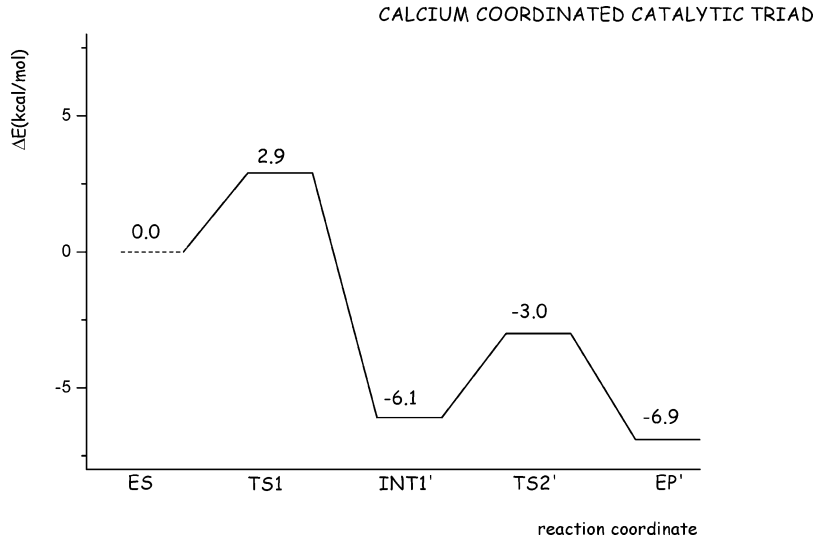

Figure 6. B3LYP potential energy surface (PES) for the calcium-coordinated catalytic triad mechanism.

TABLE 1: Effect of the Dielectric Constant on the Computed Energy Barriers for the Mechanisms A, B, and C

	A	B	C
gas phase	4.7	3.6	2.9
$\varepsilon = 2$	7.0	5.9	4.8
$\varepsilon = 4$	9.3	7.2	5.0
$\varepsilon = 40$	10.1	7.8	7.6
$\varepsilon = 80$	10.3	8.3	7.9

solvent effects could require a somewhat larger dielectric of $\varepsilon = 4$. So, we have retained as interest to see how the choice of different dielectric constant values ($\varepsilon = 2$, 4, 40, and 80) influences the energetics of the process (Table 1) for each mechanism investigated in this study.

Results reported in Table 1 indicate that energy barriers, always referred to the rate-determining step, are quite influenced by the ε values. In particular, the solvation entails that a slight increase of the energy barriers occurs. Within mechanism A (catalytic triad), the barrier increases from 7.0 ($\varepsilon = 2$) up to 10.3 ($\varepsilon = 80$) kcal/mol. As far as mechanism B (calcium-coordinated oxyanion) is concerned, a slight increase due to the solvation is also found for the cleavage of the C−O bond. Finally, in the mechanism C (calcium-coordinated catalytic triad) the barrier is found to be 4.8, 5.0, 7.6, and 7.9 kcal/mol, for $\varepsilon = 2$, 4, 40, and 80, respectively.

Although barriers are found to be larger with respect to the gas-phase ones, they remain low enough to make feasible the catalytic events also in solvent. The values computed for $\varepsilon = 2$ and $\varepsilon = 4$ are those that suit better the above-mentioned criterion suggesting 2−3 kcal/mol as maximum difference between barriers in gas phase and in solvent.

However, the lack of precise experimental information does not allow us to determine which results are the most reliable ones. In fact, few experimental studies on the determination of PLA_2 kinetic data are available in the literature. For the hydrolysis of 1,2-dioctanoyl-*sn*-glycero-3-phosphocholine micelles,[89] the rate constant was computed to be 675 s^{-1}. Wild-type bee venom PLA_2 hydrolysis of DMPM in the scooting mode at pH 8 with inhibition by HK-32 yielded to a rate constant of 130 s^{-1}.[90] Finally, a rate constant of 500 s^{-1} with the micellar substrate diC8PC (10 mM) at pH 8.0 and 25 °C for wild-type PLA2,[91] was found. These data could correspond to an activation energy of around 12−15 kcal/mol.

Since, for systems containing transition metals, B3LYP has an estimated error on relative energies of 3−5 kcal/mol,[92] one may conclude that, considering this margin of error, the results obtained here with $\varepsilon = 40/80$ seem to be nearer to the literature indication, assuming that substrate binding and/or product release are not rate determining.

Furthermore, it is noteworthy that, due to the complexity of the environment represented by the lipid−water interface in which PLA_2 operates, it is probable that the continuum method applied to study the solvent effects in this case could not be appropriate.

Conclusions

In this paper, density functional theory has been employed to investigate the two proposed catalytic mechanisms for calcium-containing phospholipase A2 enzyme, i.e., the catalytic triad and the calcium-coordinated oxyanion mechanisms. The former entails that a water molecule (W1) in the calcium outer sphere performs the tetrahedral intermediate formation by nucleophilic attack on the carbonyl carbon of the *sn*-2 ester group of the substrate, which collapses into products through protonation by His48. The latter mechanism identifies as nucleophilic agent another water molecule (W2) coordinated to calcium, and the protonation of the intermediate is performed by His48 with the intermediation of the outer W1.

Quantum chemical models have been employed to optimize intermediates and transition states for the two entire reaction mechanisms.

Calculations point out that in the first proposed mechanism, the rate-limiting step may be recognized in the W1 attack on substrate carbon atom, with an energy barrier of 4.7 kcal/mol, while protonation by His48 of tetrahedral intermediate requires a lesser amount of energy. Computations regarding the calcium-coordinated oxyanion mechanism provide that the rate-determining process lies in the decomposition of the tetrahedral intermediate that occurs into two different steps, C−O bond cleavage, yielding to an alcoholate, and its protonation by His48 with the assistance of W1. W2 nucleophilic addition is indeed very feasible.

A third mechanism proposed in this paper (named calcium-coordinated catalytic triad mechanism), which provides for calcium-bound water molecule W2 in performing the nucleophilic attack and for the only involvement of His48 without the assistance of W1 in tetrahedral intermediate protonation, yields another convincing reaction energy profile in which both

processes, formation of the intermediate and its decomposition, require low barriers to occur.

The significant involvement of the Asp99 and His48 residues in the catalysis as well as the key role played by W1 and W2 water molecules are clearly revealed. His48 constitutes the catalytic base in all reaction mechanisms, performing W1/W2 deprotonation, and consequently the nucleophile agent generation. Its base character is enhanced by the interaction with Asp99 amino acid. W2 seems to be a better nucleophile with respect to W1 because of its coordination to Ca^{2+} cation, while W1 acts in mediating W2 deprotonation and in stabilizing transition states and intermediates during catalysis.

The calcium cofactor seems to function in binding and polarizing the carbonyl group of the substrate and in providing the better nucleophile, so that a direct involvement in catalysis is revealed.

The catalytic mechanism proposed in our study may be regarded with confidence as another reliable reaction path followed by phospholipase A_2 enzyme.

Solvent effects, estimated by applying the continuum polarizable method, depend quite on the dielectric constant values. As a common aspect, we can observe that, for all considered media and irrespective of the followed mechanism, the process in the solvent appears to be slightly unfavored from both kinetic and thermodynamic points of view. However, these latter results should be taken with caution since the used approximation for the environment could not be so right to describe the complexity of the lipid−water interface where PLA_2 acts.

Acknowledgment. The University of Calabria and MIUR (PRIN 2008) are gratefully acknowledged for financial support.

References and Notes

(1) Verheij, H. M.; Slotboom, A. J.; de Haas, G. H. *Rev. Physiol. Biochem. Pharmacol.* **1981**, *91*, 91.
(2) Bayburt, T.; Gelb, M. H. *Biochemistry* **1997**, *36*, 3216.
(3) Leslie, C. C. *J. Biol. Chem.* **1997**, *272*, 16709.
(4) Higgs, H. N.; Glomset, A. A. *J. Biol. Chem.* **1996**, *271*, 10874.
(5) Berg, O. G.; Cajal, Y.; Butterfoss, G. L.; Grey, R. L.; Alsina, M. A.; Yu, B.-Z.; Jain, M. K. *Biochemistry* **1998**, *37*, 6615.
(6) Sarda, L.; Desnuelle, P. *Biochim. Biophys. Acta* **1958**, *30*, 513.
(7) Volwerk, J. J.; Filthuth, E.; Griffith, O. H.; Jain, M. K. *Biochemistry* **1994**, *33*, 3464.
(8) Lewis, A. A.; Garigapati, V. AR.; Zhou, C.; Roberts, M. F. *Biochemistry* **1993**, *32*, 8836.
(9) Griffith, O. H.; Ryan, M. *Biochim. Biophys. Acta* **1999**, *1441*, 237.
(10) Boguslavsky, V.; Rebecchi, M.; Morris, A.; John, D. Y.; Rhee, S. G.; McLaughlin, S. *Biochemistry* **1994**, *33*, 3032.
(11) Williams, R. L. *Biochim. Biophys. Acta* **1999**, *1441*, 255.
(12) Barnett, S. F.; Ledder, L. M.; Stirivant, S. M.; Ahern, J.; Conroy, R. R.; Heimbrook, D. C. *Biochemistry* **1995**, *34*, 14254.
(13) Burden, L. M.; Rao, V. D.; Murray, D.; Ghirlando, R.; Doughman, S. D.; Anderson, R. A.; Hurley, J. H. *Biochemistry* **1999**, *38*, 15141.
(14) Hurley, J. H.; Misra, S. *Annu. Rev. Biophys. Biomol. Struct.* **2000**, *29*, 49.
(15) Jain, M. K.; Krause, C. D.; Buckley, J. T.; Bayburt, T.; Gelb, M. G. *Biochemistry* **1994**, *33*, 5011.
(16) Borgstrom, B.; Brockman, H. L. *Lipase*; Elsevier: Amsterdam, 1984; p 527.
(17) Carey, M. C.; Small, D. M.; Bliss, C. M. *Annu. Rev. Physiol.* **1983**, *45*, 651.
(18) Dennis, E. A. *The Enzymes* **1983**, *16*, 307.
(19) Roberts, M. F. *FASEB J.* **1996**, *10*, 1159.
(20) Derwenda, Z. S. *Adv. Protein Chem.* **1994**, *45*, 1.
(21) Ferrato, F.; Carriere, F.; Sarda, L.; Verger, R. *Methods Enzymol.* **1997**, *286*, 327.
(22) Gelb, M. H.; Jain, M. K.; Hanel, A. M.; Berg, O. G. *Annu. Rev. Biochem.* **1995**, *64*, 653.
(23) Homan, R.; Jain, M. K. In *Intestinal Lipid Metabolism*; Mansbach, C. M., Tso, P., Kuksis, A., Eds.; Kluwer Academic Press and Plenum Publishers: New York, 2000; p 81.
(24) Richmond, B. L.; Boileau, A. C.; Zheng, S.; Huggins, K. W.; Granholm, N. A.; Tso, P.; Hui, D. Y. *Gastroenterology* **2001**, *120*, 1193.
(25) *Esterases, Lipase, and Phospholipase: from Structure to Clinical Significance*; Mackness, M. I., Clerc, M., Eds.; Plenum Press: New York, 1994; p 279.
(26) Moreau, P.; Cassagne, C. *Biochim. Biophys. Acta* **1994**, *1197*, 257.
(c) Mansbach, C. M. *J. Clin. Invest.* **1977**, *60*, 411.
(27) Smith, W. L. *Biochem. J.* **1989**, *259*, 315.
(28) Upton, C.; Buckley, J. T. *Trends Biochem. Sci.* **1995**, *20*, 178.
(29) Vrielink, A.; Lloyd, L. F.; Blow, D. M. *J. Mol. Biol.* **1991**, *219*, 533.
(30) Waite, M. *The Phospholipases*; Plenum: New York, 1987.
(31) Wittcoff, H. *The Phosphatides*; Reinhold Publishing Corp.: New York, 1951; pp 99−115.
(32) *Lipases: Their Structure, Biochemistry and Application*; Woolley, P., Petersen, S. B., Eds.; Cambridge University Press: Cambridge, UK, 1994; p 363.
(33) Jain, M. K.; Rogers, J.; Jahagirdar, D. V.; Marecek, J. F.; Ramirez, F. *Biochim. Biophys. Acta* **1986**, *860*, 435.
(34) Jain, M. K.; Maliwal, B. P.; de Haas, G. H.; Slotboom, A. J. *Biochim. Biophys. Acta* **1986**, *860*, 448.
(35) Jain, M. K.; Rogers, J.; Marecek, J. F.; Ramirez, F.; Eibl, H. *Biochim. Biophys. Acta* **1986**, *860*, 462.
(36) Jain, M. K.; de Haas, G. H.; Marecek, J. F.; Ramirez, F. *Biochim. Biophys. Acta* **1986**, *860*, 475.
(37) Jain, M. K.; Berg, O. G. *Biochim. Biophys. Acta* **1989**, *1002*, 127.
(38) Berg, O. G.; Yu, B.-Z.; Rogers, J.; Jain, M. K. *Biochemistry* **1991**, *30*, 7283.
(39) Irvine, R. F. *Biochem. J.* **1982**, *204*, 3.
(40) Ito, S.; Narumiya, S.; Hayaishi, O. *Prostaglandins, Leukotrienes Essent. Fatty Acids* **1989**, *37*, 219.
(41) Yamamoto, S. *Prostaglandins, Leukotrienes Essent. Fatty Acids* **1989**, *35*, 219.
(42) Shimizu, T.; Wolf, L. S. *J. Neurochem.* **1990**, *55*, 1.
(43) Sigal, E. *Am. J. Physiol.* **1991**, *26*, L13.
(44) Muratami, M.; Kudo, I. *J. Biochem.* **2002**, *131*, 285, and reference therein.
(45) Dijkstra, B. W.; Drenth, J.; Kalk, K. H.; Vandermaelen, P. J. *J. Mol. Biol.* **1978**, *124*, 53.
(46) Li, Y.; Tsai, M.-D. *J. Am. Chem. Soc.* **1993**, *115*, 8523.
(47) Liu, X.; Zhu, H.; Huang, B.; Rogers, J.; Yu, B.-Y.; Kumar, A.; Jain, M. K.; Sundraralingam, M.; Tsai, M.-D. *Biochemistry* **1995**, *34*, 7322.
(48) Yuan, C.; Tsai, M.-D. *Biochim. Biophys. Acta* **1999**, *1441*, 215.
(49) Einspahr, H.; Bugg, C. E. Crystal Structure Studies of Calcium Complexes and Implications for Biological Systems. In *Metal Ions in Biological Systems Vol 17; Calcium and its Role in Biology*; Sigel, H., Ed.; Marcel Dekker Inc.: New York, 1984; pp 51−97.
(50) Verheij, H. M.; Volwerk, J. J.; Jansen, E. H. J. M.; Puyk, W. C.; Drenth, J.; de Haas, G. H. *Biochemistry* **1980**, *19*, 743.
(51) Scott, D. L.; White, S. P.; Otwinowski, Z.; Yuan, W.; Gelb, M. H.; Sigler, P. B. *Science* **1990**, *250*, 1541.
(52) Thunnissen, M. G. M. M.; Ab, E.; Kalk, K. H.; Drenth, J.; Dijkstra, B. W.; Kuipers, O. P.; Dijkman, R.; de Haas, G. H.; Verheij, H. M. *Nature* **1990**, *347*, 689.
(53) Dijkstra, B. W.; Drenth, J.; Kalk, K. H. *Nature* **1981**, *289*, 604.
(54) Seshadri, K.; Vishveshwara, S.; Jain, M. K. *Proc. Indian Acad. Sci.* **1994**, *106*, 1177.
(55) Rogers, J.; Yu, B.-Z.; Serves, S. V.; Tsivgoulis, G. M.; Sotiropoulos, D. N.; Ioannou, P. V.; Jain, M. K. *Biochemistry* **1996**, *35*, 9375.
(56) Sekar, K.; Yu, B.-Z.; Rogers, J.; Lutton, J.; Liu, X.; Chem, X.; Tsai, M.-D.; Jain, M. K.; Sundaralingam, M. *Biochemistry* **1997**, *36*, 3104.
(57) Yu, B.-Z.; Rogers, J.; Nicol, G. R.; Theopold, K. H.; Seshadri, K.; Vishveshwara, S.; Jain, M. K. *Biochemistry* **1998**, *37*, 12576.
(58) Frisch, M. J.; Trucks, G. W.; Schlegel, H. B.; Scuseria, G. E.; Robb, M. A.; Cheeseman, J. R.; Montgomery, Jr., J. A.; Vreven, T.; Kudin, K. N.; Burant, J. C.; Millam, J. M.; Iyengar, S. S.; Tomasi, J.; Barone, V.; Mennucci, B.; Cossi, M.; Scalmani, G.; Rega, N.; Petersson, G. A.; Nakatsuji, H.; Hada, M.; Ehara, M.; Toyota, K.; Fukuda, R.; Hasegawa, J.; Ishida, M.; Nakajima, T.; Honda, Y.; Kitao, O.; Nakai, H.; Klene, M.; Li, X.; Knox, J. E.; Hratchian, H. P.; Cross, J. B.; Adamo, C.; Jaramillo, J.; Gomperts, R.; Stratmann, R. E.; Yazyev, O.; Austin, A. J.; Cammi, R.; Pomelli, C.; Ochterski, J. W.; Ayala, P. Y.; Morokuma, K.; Voth, G. A.; Salvador, P.; Dannenberg, J. J.; Zakrzewski, V. G.; Dapprich, S.; Daniels, A. D.; Strain, M. C.; Farkas, O.; Malick, D. K.; Rabuck, A. D.; Raghavachari, K.; Foresman, J. B.; Ortiz, J. V.; Cui, Q.; Baboul, A. G.; Clifford, S.; Cioslowski, J.; Stefanov, B. B.; Liu, G.; Liashenko, A.; Piskorz, P.; Komaromi, I.; Martin, R. L.; Fox, D. J.; Keith, T.; Al-Laham, M. A.; Peng, C. Y.; Nanayakkara, A.; Challacombe, M.; Gill, P. M. W.; Johnson, B.; Chen, W.; Wong, M. W.; Gonzalez, C.; Pople, J. A. *Gaussian 03*; Gaussian, Inc.: Pittsburgh, PA, 2003.
(59) Becke, A. D. *J. Chem. Phys.* **1993**, *98*, 5648.
(60) Lee, C.; Yang, W.; Parr, R. G. *Phys. Rev. B* **1988**, *37*, 785.
(61) Becke, A. D. *J. Chem. Phys.* **1993**, *98*, 1372.
(62) Becke, A. D. *Phys. Rev. A* **1988**, *38*, 3098.

(63) Ditchfield, R.; Hehre, W. J.; Pople, J. A. *J. Chem. Phys.* **1971**, *54*, 724.
(64) Hehre, W. J.; Ditchfield, R.; Pople, J. A. *J. Chem. Phys.* **1972**, *56*, 2257.
(65) Hariharan, P. C.; Pople, J. A. *Mol. Phys.* **1974**, *27*, 209.
(66) Gordon, M. S. *Chem. Phys. Lett.* **1980**, *76*, 163.
(67) Dolg, M.; Wedig, U.; Stoll, H.; Preuss, H. *J. Chem. Phys.* **1987**, *86*, 866.
(68) Gonzalez, C.; Schlegel, H. B. *J. Chem. Phys.* **1989**, *90*, 2154.
(69) Gonzalez, C.; Schlegel, H. B. *J. Phys. Chem.* **1990**, *94*, 5523.
(70) Siegbahn, P. E. M.; Blomberg, M. R. A. *Chem. Rev.* **2000**, *100*, 421–437.
(71) Noodleman, L.; Lovell, T.; Han, W. G.; Li, J.; Himo, F. *Chem. Rev.* **2004**, *104*, 459–508.
(72) Leopoldini, M.; Russo, N.; Toscano, M.; Dulak, M.; Wesoloski, A. T. *Chem.—Eur. J.* **2006**, *12*, 2532.
(73) Leopoldini, M.; Russo, N.; Toscano, M. *Chem.—Eur. J.* **2007**, *13*, 2109.
(74) Leopoldini, M.; Marino, T.; Russo, N.; Toscano, M. *Int. J. Quantum Chem.* **2008**, *108*, 2023.
(75) Leopoldini, M.; Chiodo, S. G.; Toscano, M.; Russo, N. *Chem.—Eur. J.* **2008**, *14*, 8674.
(76) Marino, T.; Russo, N.; Toscano, M. *J. Am. Chem. Soc.* **2005**, *127*, 4242.
(77) Leopoldini, M.; Russo, N.; Toscano, M. *J. Phys. Chem. B.* **2006**, *110*, 1063.
(78) Leopoldini, M.; Russo, N.; Toscano, M. *J. Am. Chem. Soc.* **2007**, *129*, 7776.
(79) Leopoldini, M.; Marino, T.; Toscano, M. *Theor. Chem. Acc.* **2008**, *120*, 459.
(80) Leopoldini, M.; Russo, N.; Toscano, M. *Chem.—Eur. J.* **2009**, *15*, 8026.
(81) Amata, O.; Marino, T.; Russo, N.; Toscano, M. *J. Am. Chem. Soc.* **2009**, *131*, 14804.
(82) Miertus, S.; Scrocco, E.; Tomasi, *J. Chem. Phys.* **1981**, *55*, 117.
(83) Miertus, S.; Tomasi, *J. Chem. Phys.* **1982**, *65*, 239.
(84) Cossi, M.; Barone, V.; Commi, R.; Tomasi, J. *Chem. Phys. Lett.* **1996**, *255*, 327.
(85) Barone, V.; Cossi, M.; Menucci, B.; Tomasi, J. *J. Chem. Phys.* **1997**, *107*, 3210.
(86) Cha, S. S.; Lee, D.; Adams, J.; Kurdyla, J. T.; Jones, C. S.; Marshall, L. A.; Bolognese, B.; Abdel-Meguid, S. S.; Oh, B. H. *J. Med. Chem.* **1996**, *39*, 3878.
(87) Zhao, Y.; Truhlar, D. G. *J. Phys. Chem. A* **2004**, *108*, 6908.
(88) Sekar, K.; Biswas, R.; Li, Y.; Tasi, M.-D.; Sundaralingam, M. *Acta Crystallogr.* **1999**, *D55*, 443.
(89) Dupureur, C. M.; Deng, T.; Kwak, J.-G.; Noel, J. P.; Tsai, M.-D. *J. Am. Chem. Soc.* **1990**, *112*, 7074.
(90) Annand, R. R.; Kontoyianni, M.; Penzotti, J. E.; Dudler, T.; Lybrand, T. P.; Gelb, M. H. *Biochemistry* **1996**, *35*, 4591.
(91) Janssen, M. J. W.; van de Wiel, W. A. E. C.; Beiboer, S. H. W.; van Kampen, M. D.; Verheij, H. M.; Slotboom, A. J.; Egmond, M. R. *Protein Eng.* **1999**, *12*, 497.
(92) Siegbahn, P. E. M. *J. Biol. Inorg. Chem.* **2006**, *11*, 695.

JP1003819